DIRECTIONAL COUPLERS

ABSTRACT

The directional coupler (DC) is the most useful 4-port microwave device. Substantially, it consists of a 4-port device, where a wave entering any port excites two other ports with prescribed amplitudes, whereas the remaining port is isolated. This property makes the DC an essential component when dealing with microwave devices, as it allows to distinguish reflected waves from incident ones. After a definition of the ideal DC, the typical parameters and the electrical characteristics of actual devices are illustrated, then, the main applications are considered and, finally, some common realizations of DC are shown, particularly focusing the attention on different coupling mechanisms and technologies.

DEFINITION

An ideal directional coupler is a linear, reciprocal, and lossless four-port device, often indicated as in Fig. 1, with the following properties (1):

1. The ports are matched.
2. Each port is only coupled to other two ports, the fourth one being isolated.

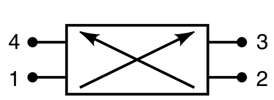

Figure 1. Schematic representations of a directional coupler.

Therefore, the scattering matrix of an ideal directional coupler takes the form

$$S = \begin{bmatrix} 0 & s_{12} & s_{13} & 0 \\ s_{12} & 0 & 0 & s_{24} \\ s_{13} & 0 & 0 & s_{24} \\ 0 & s_{24} & s_{34} & 0 \end{bmatrix} \tag{1}$$

apart from an insignificant permutation of the port indices. Thus, a wave incident at port 1, not being reflected at all, splits between port 2 and 3, while port 4 is isolated. Conversely, a wave incident at port 2 is coupled to ports 1 and 4, port 3 being isolated under that excitation (hence the name directional coupler). The fundamental parameter characterizing the ideal directional coupler is the so-called coupling, C, defined as the reciprocal of the magnitude of the transmission coefficient between ports 1 and 3 (that is, $C = -20 \log |s_{13}|$).

It is also shown that any linear, reciprocal, lossless, and matched four-port must be a directional coupler. Its scattering matrix S is in fact

$$S = \begin{bmatrix} 0 & s_{12} & s_{13} & s_{14} \\ s_{12} & 0 & s_{23} & s_{24} \\ s_{13} & s_{23} & 0 & s_{24} \\ s_{14} & s_{24} & s_{34} & 0 \end{bmatrix} \tag{2}$$

Since losslessness implies the unitarity of the scattering matrix, $SS^{+} = I$, where I is the unit matrix, the following equations must be satisfied:

$$|s_{12}|^2 + |s_{13}|^2 + |s_{14}|^2 = 1 \tag{3}$$

$$|s_{12}|^2 + |s_{23}|^2 + |s_{24}|^2 = 1 \tag{4}$$

$$|s_{13}|^2 + |s_{23}|^2 + |s_{34}|^2 = 1 \tag{5}$$

$$|s_{14}|^2 + |s_{24}|^2 + |s_{34}|^2 = 1 \tag{6}$$

$$s_{13}s_{23}^* + s_{14}s_{24}^* = 0 \tag{7}$$

$$s_{12}s_{23}^* + s_{14}s_{34}^* = 0 \tag{8}$$

$$s_{12}s_{24}^* + s_{13}s_{34}^* = 0 \tag{9}$$

By multiplying Eq. (7) by s_{12} and Eq. (8) by s_{13} and subtracting one from the other, one obtains the equation

$$s_{14}(s_{12}s_{24}^* - s_{13}s_{34}^*) = 0 \tag{10}$$

whose solutions are

$$s_{14} = 0 \tag{11}$$

$$s_{12}s_{24}^* = s_{13}s_{34}^* \tag{12}$$

Let us consider the first solution. From Eq. (7) it also follows that $s_{23} = 0$ [otherwise we would have $s_{12} = s_{13} = 0$, in contradiction with Eq. (3)]. Moreover, by subtracting Eq. (4) from Eq. (3) and Eq. (5) from Eq. (3), one obtains $|s_{13}| = |s_{24}| = \alpha$ and $|s_{12}| = |s_{34}| = \beta$. By setting $\phi_{ij} = \angle S_{ij}$, from Eq. (9) one obtains the relationship linking the phases:

$$(\phi_{12} - \phi_{13}) + (\phi_{34} - \phi_{24}) = \pi \tag{13}$$

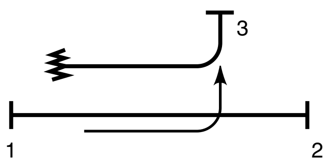

Figure 2. Schematic representations of a directional coupler in the configuration commonly used in microwave measurements.

Therefore, the scattering matrix of the device takes the form

$$S = \begin{bmatrix} 0 & \beta e^{j\phi_{12}} & \alpha e^{j\phi_{13}} & 0 \\ \beta e^{j\phi_{12}} & 0 & 0 & \alpha e^{j\phi_{24}} \\ \alpha e^{j\phi_{13}} & 0 & 0 & \beta e^{j\phi_{34}} \\ 0 & \alpha e^{j\phi_{24}} & \beta e^{j\phi_{34}} & 0 \end{bmatrix} \tag{14}$$

Note that when $\phi_{12} - \phi_{13} = \phi_{34} - \phi_{24}$, as often occurs in practical cases when the coupler is symmetrical ($s_{13} = s_{24}$ and $s_{12} = s_{34}$),

$$\phi_{12} - \phi_{13} = \pi/2 \tag{15}$$

Therefore, the outputs from ports 2 and 3 are in quadrature. In this case, it is always possible to choose the reference planes in such a way that the scattering matrix takes the form

$$S = \begin{bmatrix} 0 & j\beta & \alpha & 0 \\ j\beta & 0 & 0 & \alpha \\ \alpha & 0 & 0 & j\beta \\ 0 & \alpha & j\beta & 0 \end{bmatrix} \tag{16}$$

When we consider Eq. (12), we note immediately that the solutions $s_{12} = 0$ and $s_{34} = 0$, or $s_{13} = 0$ and $s_{24} = 0$, respectively, are the same as that obtained previously, after exchanging the coupled ports with the isolated ones. For instance, under excitation of port 1, the isolated port becomes port 2 while port 3 and port 4 are coupled. Therefore, the first case examined can be taken as typical.

An alternative picture representing a directional coupler commonly used in measurement benches is shown in Fig. 2. The figure emphasizes that port 4 of the DC is terminated on a matched load. Actually, in many applications, port 4 is not used at all. Nevertheless, this port must be loaded in order to suppress the secondary line signals due to its mismatch. Moreover, the sketch suggests an intuitive idea of the realization of a directional coupler: two parallel transmission lines electromagnetically coupled to each other. A portion of the wave traveling from port 1 toward port 2 couples to port 3. According to common parlance, the branch connecting ports 1 and 2 is called the main arm, while the one linking ports 3 and 4 is called the secondary arm.

REAL DIRECTIONAL COUPLERS

Of course, it is impossible to obtain both perfect match at the four ports and full isolation of the uncoupled ports (2,3). Therefore, in order to characterize an actual coupler, it is necessary to define, in addition to the coupling, the directivity D,

$$D = 20\log\frac{|s_{13}|}{|s_{14}|} \tag{17}$$

which represents the ratio between the power flowing from 1 to 3 and that from 1 to 4. In the ideal case the directivity is infinite. Sometimes it is preferred to use another parameter, called isolation I, defined by

$$I = 20\log\frac{1}{|s_{14}|} = C + D \tag{18}$$

Additionally, actual devices are typically characterized by the following quantities:

- *Frequency range*—Operational band of the coupler. Typically, commercial waveguide couplers operate over the whole waveguide band. Over that band the following parameters are defined:
- The nominal *coupling C*—Typical values are 3, 6, 10, 20, 30, and 40 dB.
- *Coupling sensitivity/deviation*—The maximum deviation C with respect to its nominal value.
- *Minimum directivity D*—Typically between 30 and 50 dB.
- *Insertion loss*—The maximum insertion loss on the main path (ports 1–2).
- *Primary arm VSWR*—The VSWR on the main path.
- *Secondary arm VSWR*—That of the secondary path
- *Power handling capability* (*cw*)/(*peak*)—The maximum continuous or peak power that can be carried by the coupler.
- *Connectors*—Indicate the connectors by which the coupler is fed.

MEASUREMENT OF THE COUPLER PARAMETERS

Since a directional coupler is a linear four-port device, its characteristic parameters C and D are commonly deduced by measuring the scattering parameters with the help of a network analyzer. This is very easy in coaxial and rectangular waveguides, where analyzer flanges are the same as those of the device under test. In microstrip and in planar circuits, some attention must be paid to the feed transitions. Such transitions could noticeably alter the response of the coupler. Figure 3 shows the typical measured parameters of a commercial 10-dB directional coupler in a rectangular waveguide.

APPLICATIONS

The main feature of the coupler is its ability to detect whether a wave traveling along the main branch is propagating from 1 to 2 or in the opposite direction. That makes the coupler an essential component in telecommunication and measurement systems. A few of the most important applications are discussed next.

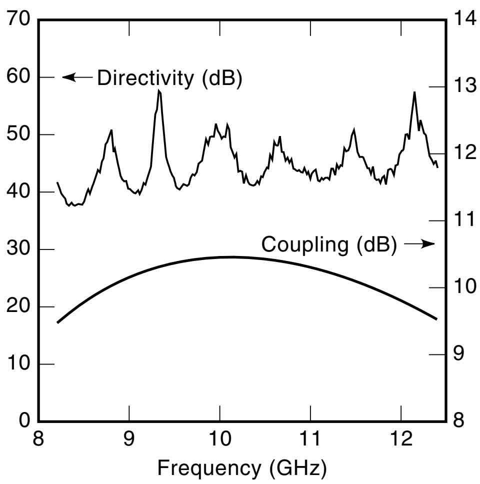

Figure 3. Coupling and directivity of a commercial 10 dB multihole waveguide directional coupler.

Reflectometer

From the detection of the propagation direction of a wave follows the possibility of measuring the reflection of an unknown device. This is achieved by arranging the measurement bench as depicted in Fig. 4.

In the ideal case [i.e., when the scattering matrix of the directional coupler is given by Eq. (1), and assuming port 4 to be perfectly matched], the signal detected at port 3, b_3, is proportional to ρ_l, the reflectivity of the device under test (DUT) loading port 1, while port 2 is fed by a microwave generator (4). In fact,

$$b_3 = s_{13}s_{12}\rho_l \tag{19}$$

The measurement requires knowledge of the term $s_{13}s_{12}$, which can be easily measured by substituting the unknown load ρ_l with a known one, typically a totally reflecting load, as a short circuit ($\rho_k = -1$). Under such a condition, the signal delivered at port 3 is

$$b_{3k} = -s_{13}s_{12} = -s_{13}s_{12} \tag{20}$$

Once this step, commonly referred to as the calibration, has been completed, one can find the reflection ρ_l as

$$\rho_l = -b_3/b_{3k} \tag{21}$$

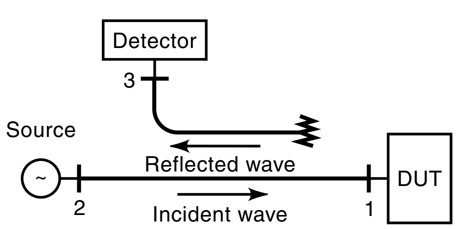

Figure 4. Bench for reflectometry measurements: By means of the DC, part of the signal reflected by the device under test flows to port 3, where it is detected and measured.

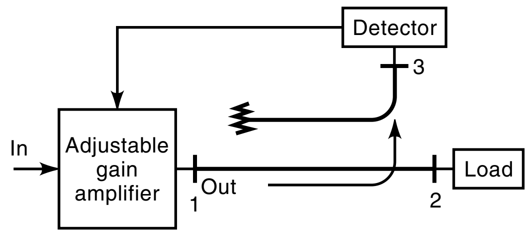

Figure 5. Monitoring and feedback of a source output: Part of the signal outgoing from the amplifier is coupled into the detector and used to control the gain of the amplifier.

Monitoring, Feedback, and Power Measurements

In the configuration of Fig. 5 the coupler is used for the purpose of monitoring the output level of a given source. The signal at port 3 can also be used as a feedback for the source itself—for instance, when a leveled output power is required (see FEEDBACK AMPLIFIERS).

The use of coupler with large coupling is very useful when dealing with measurements of high power signals, which could destroy power meters (see POWER METERS). The typical bench for such measurements is shown in Fig. 6.

Couplers as Part of More Complex Systems

The coupler often represents an essential part of more complex devices, such as the mixer (see MIXERS) or the four-way circulator (see FERRITE DEVICES), shown in Figs. 7 and 8, respectively. In the first case the coupler provides a strong separation between the local oscillator (LO), while in the second case two 3 dB couplers, connected as shown in Fig. 8, permit one to obtain (in the ideal case) the following scattering matrix:

$$S = \begin{bmatrix} 0 & 0 & 0 & e^{j\phi_{14'}} \\ 0 & 0 & e^{j\phi_{41'}} & 0 \\ 0 & e^{j\phi_{1'4}} & 0 & 0 \\ e^{j\phi_{4'1}} & 0 & 0 & 0 \end{bmatrix} \tag{22}$$

When port 1 is fed, the power equally splits between ports 2 and 3, while port 4 is isolated. Then, thanks to the phase shifter, the signal traveling from port 3 to port 3′ is shifted by 180° with respect to the signal directly arriving at port 2′. The output of the combination of the two signals 180° out of phase is different from zero only at port 4′. Therefore, $s_{14} = 0$, $s_{14'} \neq 0$ and $s_{11'} = 0$. Analogously, when port 4 is fed, ports

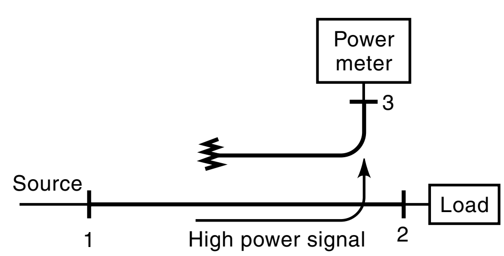

Figure 6. Measurement of power signals: Only a small amount of the power signal is delivered to the power meter in order to prevent damage.

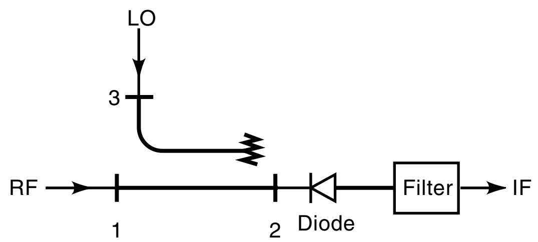

Figure 7. Microwave mixer: The radio frequency (RF) low power signal, coming from the antenna, is mixed with the one generated by the local oscillator (LO) via a nonlinear device (diode). The filter separates the intermediate frequency (IF) while the directional coupler provides a strong isolation between RF and LO channels.

1 and 4′ are isolated, while port 1′ is coupled. It is easy to repeat the same reasoning when ports 1′ and 4′ are fed and to recover the scattering matrix of Eq. (22).

COUPLING MECHANISMS

The two lengths of transmission line forming the coupler can be coupled to each other by different mechanisms. Schematically, a first distinction can be made between lumped and distributed coupling (5).

Considering that at microwave frequencies purely lumped coupling does not exist, since propagation effects occur, we will consider the coupling as lumped if the region where the coupling physically takes place is much shorter than the wavelength. Lumped coupling can be achieved both in waveguide and in planar technology.

In the first case, a further distinction can be made as to whether the coupling is directive or not. Coupling may be made directive by shaping the coupling region in such a way that on the secondary guide it produces two waves that are in phase opposition in one direction. The double aperture in-

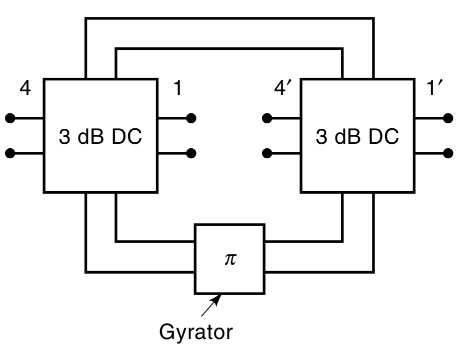

Figure 8. A 4-way circulator is supposed to feed one port at a time. For instance port 1: In that case port 4 is uncoupled and the signal is split equally among the remaining ports of the first junction. At the second junction, the two signals combine 180° out of phase because of the phase shifter inserted in the lower pattern. Therefore, due to the symmetry, they can couple only to port 4′, while port 1′ is isolated. The same reasoning applies when port 4′ is being fed. In that case, however, the phase shifter does not operate as the signal flows counterclockwise in the lower pattern. Therefore, the signals arriving at the first coupler are in phase and combine only to port 1. Analogous reasoning holds for ports 1′ and 4.

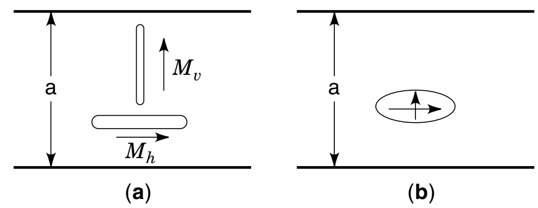

Figure 9. Riblet and Saad directional aperture: In the second arm, the magnetic current $\boldsymbol{M}_v$ excites two waves whose amplitudes are 180° out of phase and propagating in opposite directions. On the contrary, the waves excited by the magnetic current $\boldsymbol{M}_h$ are in phase. Hence, it is possible to adjust the dimensions of the apertures in such a way that the two scattered waves cancel in one direction and sum in the opposite over a broad band.

vented by Saad and Riblet (6), Fig. 9(a), provides a clear example of such a mechanism. In fact, in the secondary guide the thin vertical slot produces two waves 180° out of phase, propagating in opposite direction, while the thin horizontal slot produces two waves in phase. It is therefore possible to choose the dimensions and the positions of the two slots so that the amplitudes of the waves that are separately excited are almost the same. Thus, in one direction the two waves sum in phase while in the opposite direction they cancel. Note that the bandwidth of this coupler is wide enough since the aforementioned mechanism does not take advantage of resonance effects. The same mechanism can be exploited by collapsing the two thin apertures into an elliptical one and adjusting eccentricity and the position according to the preceding criteria (7,8), as shown in Fig. 9(b).

Of course, coupler performance can be strongly improved by cascading several properly spaced apertures. To understand the principle of operation, let us consider two lengths of rectangular waveguides positioned side by side and coupled via two apertures drilled in the broad wall, as illustrated in Fig. 10. We want to couple them in such a way that a fraction of the power traveling from port 1 to port 2 is delivered to port 3 while port 4 is isolated. On the contrary, a wave traveling from 2 to 1 must couple only to port 4. If C_k and D_k denote the fraction of signal delivered to ports 3 and 4, respectively,

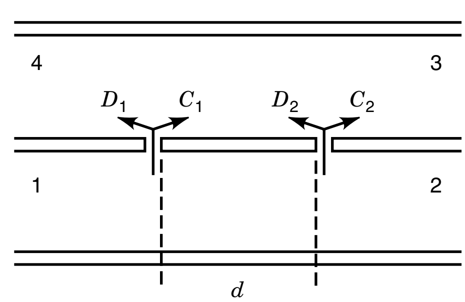

Figure 10. Waveguides coupled via two circular holes spaced by a distance $d = \lambda_g/4$. At the resonant frequency the waves propagating toward the right, C_1 and C_2, coupled to the secondary arm by the holes, sum in phase while those propagating toward the left, D_1 and D_2, cancel, because of the 180°-phase shift due to the different pattern.

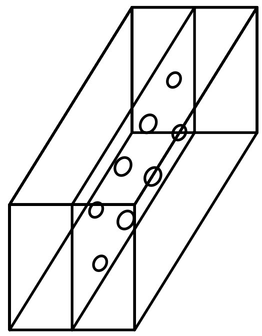

Figure 11. Multiaperture waveguide directional coupler: Dimensions and positions of the coupling holes are chosen so as to optimize DC performance over the whole waveguide band.

when a wave travels from port 1 to 2, then the amplitude of the wave at port 3 is given by

$$A_3 \approx |(C_1 + C_2)| \tag{23}$$

while at port 4 we have

$$A_4 \approx |(D_1 + D_2 e^{-j2\beta d})| \tag{24}$$

Therefore, if $D_1 \approx D_2$, $C_1 \approx C_2$, and $2\beta d = \pi$ (that is, the apertures are equal and spaced by $\lambda g/4$), $A_4 = 0$. Hence, the structure shows, at least at one frequency, the characteristics we are looking for. It is apparent that the design of a directional coupler providing given performance over almost the whole waveguide band is quantitatively much more complicated and requires the use of an appropriately dimensioned array of apertures, as schematically sketched in Fig. 11.

Under the hypothesis that the power coupled by a single aperture to the secondary waveguide is small, let us assume C_n and D_n to be the coupling coefficients of the nth aperture in the forward and reverse directions. Let us also suppose to separate the apertures by a distance d. Hence, the whole coupling into port 3, B_3, computed in correspondence of the last aperture, is

$$B_3 = Ae^{-j\beta Nd} \sum_{n=0}^{N} C_n e^{-j\beta(N-n)d} \tag{25}$$

The whole coupling coefficient into port 4, B_4, computed in correspondence of the first aperture is

$$B_4 = A \sum_{n=0}^{N} D_n e^{-j2\beta nd} \tag{26}$$

Coupling and directivity are given by the following formulas (2):

$$C = -20 \log \left| \sum_{n=0}^{N} C_n \right| \tag{27}$$

$$D = -C - 20 \log \left| \sum_{n=0}^{N} D_n e^{-j2\beta nd} \right| \tag{28}$$

Bethe showed that the forward and the reverse couplings between two waveguides via a circular aperture of radius r_n, normalized with respect to the waveguide width a, are, respectively, $C_n = T_f r_n^3$ and $D_n = T_b r_n^3$. Under the hypothesis that the wall separating the two waveguides is infinitesimally thin, the coefficients T_f and T_b assume closed-form expressions (9). Therefore, we can rewrite C and D in terms of the latter:

$$C = -20 \log |T_f| - 20 \log \left| \sum_{n=0}^{N} r_n^3 \right| \tag{29}$$

$$D = -C - 20 \log |T_b| - 20 \log |F| \tag{30}$$

where we have used the array factor F, defined as $F = \sum_{n=0}^{N} r_n^3 e^{-j2\beta nd}$.

The radii r_n are then chosen in such a way as to obtain C and D over the prescribed band. This is analogous to the design of filters and impedance transformers. As in those cases, a Chebyshev characteristic often represents the best tradeoff in terms of performance/number of array elements. Apertures are chosen in such a way as to equate the coefficients of the array factor to those of the Chebychev polynomial of order N, T_N.

$$F = \left| \sum_{n=0}^{N} r_n^3 e^{-j2n\theta} \right| = K |T_N(\sec\theta_m \cos\theta)| \quad \text{where } \theta = \beta d \tag{31}$$

The midband frequency is $\theta = \pi/2$ and corresponds to $d = \lambda_g/4$, and θ_m is the value of βd at the band edges. The positive constant K is chosen to obtain the desired coupling at the midband frequency:

$$C = -20 \log K |T_f| |T_N(\sec\theta_m)| \tag{32}$$

When $\theta = 0$, $F = |\sum_{n=0}^{N} r_n^3| = |T_N(\sec\theta_m)|$. Therefore, the directivity is given by the formulas

$$D = 20 \left[\log \left| \frac{T_f}{T_b} \right| + \log \left| \frac{T_N(\sec\theta_m)}{T_N(\sec\theta_m \cos\theta)} \right| \right] \theta \neq \frac{\pi}{2} \tag{33}$$

$$D = 20 \left[\log \left| \frac{T_f}{T_b} \right| + \log |T_N(\sec\theta_m)| \right] \theta = \frac{\pi}{2} \tag{34}$$

Although T_f/T_b depends on frequency and the characteristic is, in principle, different from the Chebyshev one, nevertheless such a shift is almost negligible, except very close to the midband frequency. Therefore, in the wideband case that contribution is negligible in the band where $\beta d = \theta_m$. Correspondingly,

$$D = D_m = 20 \log |T_N(\sec\theta_m)| \tag{35}$$

where D_m is the minimum directivity in the passband, due to the array factor. Hence, once the coupler specifications are set in terms of midband frequency $f0$, bandwidth Δ_f, coupling, and directivity, the distance d separating two adjacent apertures is given by

$$d = \frac{\pi}{2\beta(f0)} \tag{36}$$

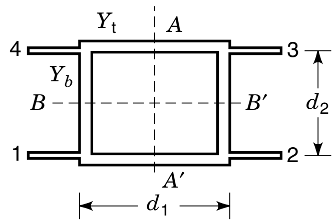

Figure 12. The branch line coupler.

It is immediate to compute cos $\theta_m \approx d\beta(f0 \pm \Delta f)$ and, from Eq. (35), the degree N of the Chebyshev polynomial yielding the specifications on directivity. Because of the nonlinearity of $\beta(f)$, cos θ_m is only approximatively calculated.

The constant K is obtained from Eq. (32):

$$K = 10^{-C/20}\left|T_f\right|\left|T_N(\sec\theta_m)\right| \tag{37}$$

Once the coefficients T_f are properly computed, either by means of an electromagnetic analysis or by Bethe's more accurate closed formulas, one has only to equate the coefficients of the array factor to those of T_N and to determine the aperture radii. The preceding theory could be further improved with the help of a more accurate analysis of the coupling mechanisms, as the one proposed by Levy (10,11). At present, however, thanks to the availability of efficient and accurate field theory based computer aided design (CAD), it seems to be more convenient to improve the design by performing an optimization directly on the electromagnetic model of the actual physical structure. The resulting design is exact, and device tuning is unnecessary (12) (see ELECTROMAGNETIC FIELD MEASUREMENT) (13).

In planar technology, lumped coupling is often obtained by physically connecting two lines. In the preceding configuration, coupling due to electromagnetic induction can be considered negligible with respect to direct coupling. The main couplers employing such a coupling mechanism are the branch line coupler and the hybrid ring coupler. Both permit one to obtain large coupling values easily, since the lines are electrically connected. In particular, the electromagnetic analysis of the first one (Fig. 12) is difficult to carry out rigorously; a circuit analysis, however, is simple if one takes advantage of the 4-fold symmetry. In fact, it is easy to study the equivalent circuit under four independent excitations: (1,1,1,1), (1,−1,−1,1), (1,−1,1−1), (1,1,−1,−1). The corresponding reflections at the port 1, Γ_a, Γ_b, Γ_c, Γ_d are given by (5)

$$\Gamma_a = \frac{1 - jY_t t_t - jY_b t_b}{1 + jY_t t_t + jY_b t_t} \tag{38}$$

$$\Gamma_b = \frac{t_t + jY_t - jY_b t_t t_b}{t_t - jY_t + jY_b t_t t_b} \tag{39}$$

$$\Gamma_c = \frac{t_b - jY_t t_t t_b + jY_b}{t_b + jY_t t_t t_b - jY_b} \tag{40}$$

$$\Gamma_d = \frac{t_t t_b + jY_t t_b + jY_b t_t}{t_t t_b - jY_t t_b - jY_b t_t} \tag{41}$$

where t_t = tan $\beta_t d_1/2$, t_b = tan $\beta_d d_2/2$, and Y_t and Y_b are the normalized characteristic admittances of the through and of the branch lines, respectively. The characteristic admittance of the input line is normalized to 1.

It is immediate to combine Eqs. (38–41), thus finding the scattering parameters of the branch line coupler:

$$S_{11} = \frac{1}{4}(\Gamma_a + \Gamma_b + \Gamma_c + \Gamma_d) \tag{42}$$

$$S_{12} = \frac{1}{4}(\Gamma_a - \Gamma_b + \Gamma_c - \Gamma_d) \tag{43}$$

$$S_{13} = \frac{1}{4}(\Gamma_a - \Gamma_b - \Gamma_c + \Gamma_d) \tag{44}$$

$$S_{14} = \frac{1}{4}(\Gamma_a + \Gamma_b - \Gamma_c - \Gamma_d) \tag{45}$$

If $t_t = t_b = 1$ (that is, the electrical lengths of the through and the branch lines are the same) and also $Y_t^2 - Y_b^2 = 1$, the four ports are matched, $S_{14} = 0$, and

$$S_{31} = -\frac{Y_b}{Y_t} \tag{46}$$

$$S_{21} = -j\frac{1}{Y_t} \tag{47}$$

S_{31} and S_{21} are in quadrature, which is predictable because of the symmetry of the coupler. The coupling C = 20 log $1/|S_{31}|$ depends on the ratio between the two characteristic impedances. When $Y_t/Y_b = \sqrt{2}$, C = 3 dB. In that case a coupler, also having the outputs in quadrature, is commonly called hybrid. The preceding characteristics hold exactly only in a narrow interval around of the working frequency. However, it is possible to enlarge considerably the bandwidth of the coupler by cascading sections (14,15).

The principal of operation of the hybrid ring (Fig. 13) is similar to that of the branch coupler. When port 1 is fed, the signal splits equally into two signals traveling clockwise and counterclockwise that recombine at the remaining ports. At ports 2 and 3 the signals sum in phase, while at port 4 they are 180° out of phase and their combination is negligible. Therefore, ports 2 and 3 are coupled while port 4 is isolated. The reasoning can be easily extended to the other ports, thus recovering the characteristic of a DC.

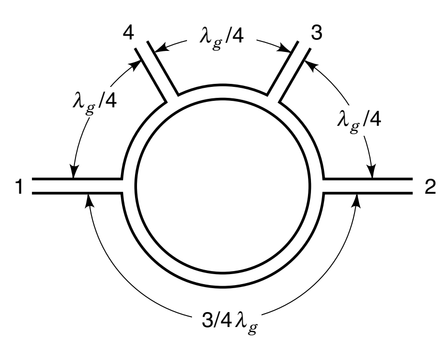

Figure 13. Ring coupler: A wave entering port 1 is split into two waves that recombine in phase at ports 2 and 4. On the other hand, port 3 is isolated, since the waves propagating clockwise and counterclockwise respectively are 180° out of phase. The same reasoning applies to the remaining ports.

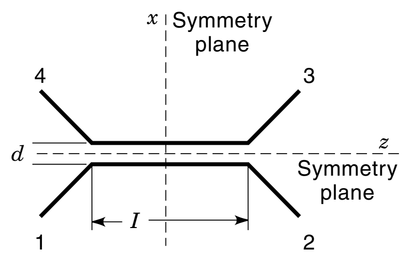

Figure 14. Distributed coupling between strips on the same substrate: A wave travelling on a line couples electromagnetically to the other one. Coupling depends both on the distance between the lines and on their length.

DISTRIBUTED COUPLING

In planar structures (e.g., microstrip, stripline, finline, slotline, which are the most common), as well as in TEM lines (e.g., coaxial cables), the coupling is often obtained by placing the two lines parallel and close to each other over a certain length, in such as way that a portion of the field wave traveling along the first guide couples by electromagnetic induction into the second one in contraflow, as schematically schetched in Fig. 14 (16–18). The coupling depends mainly on the gap separating the two strips: The wider the gap, the weaker the coupling.

We take as typical the coupler shown in Fig. 14 consisting of two parallel strips of length l placed on a grounded substrate and separated by a distance d. The twofold symmetry of the circuit with respect to the planes $x = 0$ and $z = 0$ enforces the following relationships linking the scattering parameters:

$$s_{11} = s_{22} = s_{33} = s_{44} \tag{48}$$

$$s_{12} = s_{34} \tag{49}$$

$$s_{13} = s_{24} \tag{50}$$

$$s_{14} = s_{23} \tag{51}$$

Hence, the scattering matrix takes the form

$$S = \begin{bmatrix} s_{11} & s_{12} & s_{13} & s_{14} \\ s_{12} & s_{11} & s_{14} & s_{13} \\ s_{12} & s_{14} & s_{11} & s_{14} \\ s_{14} & s_{13} & s_{12} & s_{11} \end{bmatrix} \tag{52}$$

The scattering parameters can be calculated by considering two independent sets of excitations. The first is $a_1 = 1$, $a_2 = 0$, $a_3 = 0$, $a_4 = 1$ and corresponds to a magnetic wall on the symmetry plane $x = 0$. The second is $a_1 = 1$, $a_2 = 0$, $a_3 = 0$, $a_4 = -1$ and corresponds to an electric wall on the same symmetry plane. The reflected waves at ports 1 and 2 are given by

a under the first excitation

$$b_1^e = s_{11} + s_{13} \tag{53}$$

$$b_2^e = s_{12} + s_{14} \tag{54}$$

b under the second excitation

$$b_1^o = s_{11} - s_{13} \tag{55}$$

$$b_2^o = s_{12} - s_{14} \tag{56}$$

It is immediate to calculate the parameters of the four-port:

$$s_{11} = \frac{b_1^e + b_1^o}{2} \tag{57}$$

$$s_{12} = \frac{b_2^e + b_2^o}{2} \tag{58}$$

$$s_{13} = \frac{b_1^e - b_1^o}{2} \tag{59}$$

$$s_{14} = \frac{b_2^e - b_2^o}{2} \tag{60}$$

The preceding two situations can be modeled by two transmission lines having normalized characteristic impedances Z_0^e and Z_0^o and, correspondingly, electrical lengths θ^e and θ^o. Although the physical lengths of the lines are the same, their electrical lengths are different in the non-TEM case, and the propagation constants are different in the two cases. Let us suppose both lines are fed by transmission lines with unit characteristic impedance. The transmission matrices are given by

$$T = \begin{bmatrix} \cos\theta^{e/o} & jZ_0^{e/o}\sin\theta^{e/o} \\ \dfrac{j}{Z_0^{e/o}}\sin\theta^{e/o} & \cos\theta^{e/o} \end{bmatrix} \tag{61}$$

As observed previously, losslessness implies that the condition under which the device is a directional coupler is $s_{11} = 0 = b_1^e + b_1^o$. Such a condition is satisfied when

$$\frac{\left(Z_0^e - \dfrac{1}{Z_0^e}\right) j\sin\theta^e}{2\cos\theta^e + \left(Z_0^e + \dfrac{1}{Z_0^e}\right) j\sin\theta^e} = \frac{\left(Z_0^o - \dfrac{1}{Z_0^o}\right) j\sin\theta^o}{2\cos\theta^o + \left(Z_0^o + \dfrac{1}{Z_0^o}\right) j\sin\theta^o} \tag{62}$$

An immediate solution is obtained when $\theta^e = \theta^o = \theta$, as occurs when the strips are embedded in a homogeneous medium, and $Z_0^o = 1/Z_0^e$. The more immediate solution is therefore to place over the strip a dielectric layer that has the same permittivity as the substrate. This particular case pertains to TEM couplers. In such a case, the coupling C is given by the formula

$$C = 20\log\frac{[1 - c^2\cos^2\theta]^{1/2}}{c\sin\theta} \tag{63}$$

where $c = Z_0^e - Z_0^o/Z_0^e + Z_0^o$. Since in microstrip technology $c_{\max} \approx \frac{1}{2}$, the maximum coupling achievable by the ordinary photolithographic technique is about 6 dB and occurs when $\theta = \pi/2$. Moreover, its bandwidth is rather narrow and the

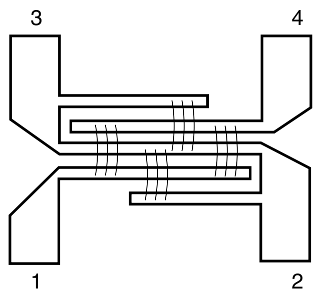

Figure 15. Lange interdigitated coupler. Bond wire connects strips to suppress the propagation of unwanted modes.

directivity moderate. Much better performances are obtained by the Lange interdigitated coupler, shown in Fig. 15 (19).

This configuration permits one to achieve 3 dB coupling easily, as well as an octave bandwidth and a good directivity. This coupler is, however, difficult to realize and the bond wires are critical at the higher frequencies. Moreover, the higher the frequency, the more difficult it is to equalize the phase velocities of the even and odd modes. Nevertheless, its good electrical characteristics and compactness make the Lange coupler suitable for applications up to 30 GHz with standard technology, but the gallium arsenide (GaAs) monolithic version is used up to 100 GHz. A comprehensive and accurate analysis of the interdigited coupler is reported in Ref. 20.

The compensation of the different phase velocities over a wide band is one of the more difficult tasks in microstrip couplers. At present, designers often adopt one of the following strategies:

1. Placing two capacitances across the lines at the input and the output
2. Using nonuniform planar transmission lines
3. Shaping the two strips in a serpentine form or in a shark-teeth form (wiggly coupler) as shown in Fig. 16.
4. Combining the preceding techniques (for instance, by shaping as shark teeth the strips of a nonuniform coupler)

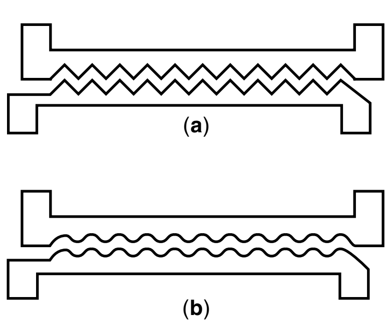

Figure 16. The wiggly and serpentine coupler. These configurations are meant to equalize even the odd phase velocities, in order to optimize the coupler response over a wide band.

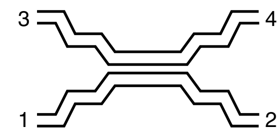

Figure 17. An example of a multisection microstrip coupler.

Similar to waveguide couplers, bandwidth and directivity can be much improved by cascading many coupled line sections, as indicated in Fig. 17 (21–23).

A detailed description of planar directional couplers can be found in Ref. 24. Planar couplers are also affected by high conductor losses. In this regard, the use of superconductor technology is attractive, though unfortunately not mature enough for large-scale production. Microstrip couplers do not achieve performances comparable to the ones realized in waveguide; therefore, they are hardly employed in measurement benches, where high directivity and loss losses are required. However, their use in civil telecommunication systems is widespread.

BIBLIOGRAPHY

1. S. B. Cohn and R. Levy, History of microwave passive components with particular attention to directional couplers, *IEEE Trans. Microw. Theory Tech.,* **32**: 1046, 1054, 1984.
2. R. Collin, *Field Theory of Guided Waves,* 2nd ed., Piscataway, NJ: IEEE Press, 1992.
3. K. Chang, *Handbook of Microwave Components, Microwave Passive Components and Antennas,* Vol. 1, New York: Wiley, 1990.
4. T. S. Laverghetta, *Modern Microwave Measurements and Techniques,* Norwood, MA: Artech House, 1988.
5. R. Collin, *Foundations for Microwave Engineering,* 2nd ed., New York: McGraw-Hill, 1992.
6. H. J. Riblet and T. S. Saad, A new type of waveguide directional coupler, *Proc. IRE,* **36**: 61–64, 1948.
7. R. Levy, Directional couplers. In *Advances in Microwaves,* Vol. 1, New York: Academic Press, 1966, pp. 115–206.
8. G. L. Matthaei, L. Young, and E. M. T. Jones, *Microwave Filter, Impedance Matching Networks and Coupling Structures,* New York: McGraw-Hill, 1964.
9. H. Bethe, Theory of diffraction by small holes, *Phys. Rev.,* **66**: 163–182, 1944.
10. R. Levy, Analysis and synthesis of waveguide multi-aperture directional couplers, *IEEE Microw. Theory Tech.,* **16**: 995–1006, 1968.
11. R. Levy, Improved single and multi-aperture waveguide coupling theory, including explanation of mutual interactions, *IEEE Microw. Theory Tech.,* **28**: 331–338, 1980.
12. P. Arcioni et al., Wideband modeling of arbitrarily shaped E-plane waveguide components by the boundary integral-resonant mode expansion method, *IEEE Microw. Theory Tech.,* **44**: 1017–1023, 1996.
13. J. Uher, J. Bornemann, and U. Rosenberg, *Waveguide Components for Antenna Feed Systems: Theory and CAD,* Norwood, MA: Artech House, 1993.
14. R. Levy and L. F. Lind, Synthesis of symmetrical branch guide directional couplers, *IEEE Microw. Theory Tech.,* **16**: 80–89, 1968.
15. R. Levy, Zolotarev branch guide directional couplers, *IEEE Microw. Theory Tech.,* **21**: 95–99, 1973.

16. J. A. G. Malherbe, *Microwave Transmission Line Couplers,* Norwood, MA: Artech House, 1988.
17. B. Bhat and S. K. Koul, *Analysis Design and Applications of Fin Lines,* Norwood, MA: Artech House, 1987.
18. K. C. Gupta et al., *Microstrip Lines and Slotlines,* Norwood, MA: Artech House, 1996.
19. J. Lange, Interdigitated stripline quadrature hybrid, *IEEE Trans. Microw. Theory Tech.,* **17**: 1150–1151, 1969.
20. V. Rizzoli and A. Lipparini, The design of interdigitated couplers for MIC applications, *IEEE Trans. Microw. Theory Tech.,* **26**: 7–15, 1978.
21. R. Levy, General synthesis of asymmetrical multi-element coupled-transmission-line directional couplers, *IEEE Microw. Theory Tech.,* **11**: 226–237, 1963.
22. E. G. Crystal and L. Young, Theory and tables of optimum symmetrical TEM-mode directional couplers, *IEEE Microw. Theory Tech.,* **13**: 544–558, 1965.
23. P. P. Toulios and A. C. Todd, Synthesis of symmetrical TEM-mode directional couplers, *IEEE Microw. Theory Tech.,* **13**: 536–543, 1965.
24. S. Uysal, *Nonuniform Line Microstrip Directional Couplers and Filters,* Norwood, MA: Artech House, 1993.

TULLIO ROZZI
ANTONIO MORINI
Università di Ancona

DIRECTIONAL COUPLERS. See ATTENUATORS.

DIRECTION FINDING, RADIO. See RADIO DIRECTION FINDING.